CHARACTERIZING THE THERMAL EFFECTS OF HIGH ENERGY ARC FAULTS

Anthony Putorti[1], Nicholas B. Melly[2], Scott Bareham[1], Joseph Praydis Jr.[1]

[1] National Institute of Standards and Technology (NIST), Gaithersburg, MD, USA
[2] U.S. Nuclear Regulatory Commission (NRC), Washington, DC, USA*

ABSTRACT

International and domestic operating experience involving High Energy Arc Faults (HEAF) in Nuclear Power Plant (NPP) electrical power systems have demonstrated the potential to cause extensive damage to electrical components and distribution systems along with damage to adjacent equipment and cables. An international study by the Committee on the Safety of Nuclear Installations (CSNI) "OECD Fire Project – Topical Report No. 1: Analysis of High Energy Arcing Fault (HEAF) Fire Events" published June 25, 2013 [1], illustrates that HEAF events have the potential to be major risk contributors with significant safety consequences and substantial economic loss. In an effort to better understand and characterize the threats posed by HEAF related phenomena, an international project has been chartered; the Joint Analysis of Arc Faults (Joan of ARC) OECD International Testing Program for High Energy Arc Faults. One of the major challenges of this research is how to properly measure and characterize the risk and influence of these events. Methods are being developed to characterize relevant parameters such as; temperature, heat flux, and heat release rate of fires resulting from HEAF events. Full scale experiments are being performed at low (≤ 1000 V) and medium (≤ 35 kV) voltages in electrical components. This paper introduces the methods being developed to measure thermal effects and discusses preliminary results of full scale HEAF experiments.

INTRODUCTION

Switchgear, load centers, and bus bars/ducts (440 V and above) are subject to a unique failure mode and, as a result, unique fire characteristics. In particular, these types of high-energy electrical devices are subject to high-energy arcing fault (HEAF). This fault mode leads to the rapid release of electrical energy in the form of heat, vaporized copper/aluminum, and mechanical force. Faults of this type are also commonly referred to as high energy, energetic, or explosive electrical equipment faults or fires.

The energetic fault scenario typically consists of two distinct phases, each with its own damage characteristics. The first phase is characterized by a short, rapid release of electrical energy which may result in catastrophic failure of the electrical enclosure, ejection of hot projectiles (from damaged electrical components or housing) and/or fire(s) involving the electrical device itself, as well as any external exposed combustibles, such as overhead exposed cable trays or nearby panels, that may be ignited during the energetic phase. The second phase, i.e., the ensuing fire(s) typically includes ignition of combustible material within the HEAF zone of influence (ZOI). The resulting fire may be due to the ejection of hot particles or piloted ignition of combustibles. HEAF events are of concern due to their potential to im-

* This paper was prepared (in part) by employees of the United States Nuclear Regulatory Commission. It presents information related to NRC upcoming testing programs. NRC has neither approved nor disapproved its technical content. This paper does not establish an NRC technical position.

pact adjacent items important to safety and current limitations in characterizing the ZOI as defined in NUREG/CR-6850 [2].

Due to the potential safety significance of HEAF events, the OECD (*O*rganization for *E*conomic *C*o-operation and *D*evelopment) Nuclear Energy Agency (NEA) Integrity and Ageing Working Group (IAGE) initiated a task on High Energy Arcing Events (HEAF) in 2009 to provide an in-depth investigation on HEAF events in NEA member states [3]. The objective of this working group is to determine damage mechanisms, extent of areas affected, methods of protecting systems, structures and components (SSC) and possible calculation methods for modeling of HEAF events as applicable to fire protection in nuclear power plants (NPP). As part of this effort a testing program has been initiated to investigate the HEAF fire phenomena to inform future deterministic and probabilistic methods.

This paper presents methods for measuring the heat release rates of ensuing fires and measuring the heat fluxes above and around the electrical enclosures during the HEAF experimental program. Limited data are also presented.

BACKGROUND

In order to characterize the effects of the HEAF and ensuing fire on the surrounding equipment, various phenomena were chosen for characterization in the OECD program. These include enclosure pressure, enclosure surface temperature, heat release rate, and heat flux to target equipment. Electrical test parameters such as arc voltage, arc current, and arc duration were also measured during the experiments.

Experiments were performed at KEMA-Powertest, located outside of Philadelphia, Pennsylvania, USA. The test facility includes a five-sided test cell approximately 8 m (26 ft) high, 7 m (24 ft) deep, and 9 m (29 ft) wide. The sixth side of the test cell includes a roll-up door that was fully open during the experiments. Bus bar connections for supplying low and medium voltage test current are located on opposite side walls of the test cell. KEMA-Powertest provided measurements of electrical enclosure pressure, temperatures of slug calorimeters, electrical test parameters, videography, and high speed videography during the experiments. NIST provided measurements of heat release rate, heat flux, electrical enclosure surface temperature, thermal imaging, and multiple location videography during the experiments.

The NPP equipment for the experiments was provided by OECD/NEA HEAF Project partners. Fourteen experiments have been performed to date using six electrical enclosures. Nominal test voltages ranged from 480 VAC to 7200 VAC, and nominal test currents ranged from 24 kA to 50 kA. All of the experiments conducted thus far have been performed with three phase power supplied in a delta configuration. The arcs were initiated in the enclosures by shorting across all three bus bar phases with a 2.6 mm diameter (10 AWG) tinned copper stranded wire prior to energizing the enclosures.

EXPERIMENTAL METHODS

Heat Release Rate

In order to measure the heat release rate (HRR) of the ensuing fires caused by the HEAF events, a portable oxygen consumption heat release rate hood apparatus was deployed. The portable hood was first used in the HELEN-FIRE experiments to measure the heat release rates of fires in control cabinets as described in NUREG/CR-7197 [4]. The portable apparatus was further developed and refined for use in the HEAF experiments. In the current form, the apparatus is a portable stand-alone system resistant to the effects of electromagnetic interference (EMI).

The portable hood, installed in the HEAF test cell with an electrical enclosure, is shown in Figure 1 and Figure 2. The hood was approximately 2.44 m by 2.44 m in width, with a clear height of approximately 3.0 m above the floor. Side skirts constructed of fiberglass welding curtain hung around the hood opening to reduce the quantity of smoke that escaped from the sides of the hood.

The exhaust duct exiting the top of the hood is approximately 0.46 m in diameter, and carries air and combustion products through flow measurement, gas sampling, and exhaust fan sections. The ducting is supported by scaffolding (not shown). The distance between the hood and the flow measurement section was varied with additional duct sections (not shown) to provide adequate clearance between the electrical enclosures and the metal scaffolding. The hood exhaust fan motor was powered by a dedicated portable electrical generator located outside of the test cell. The gas analyzers and data acquisition system were located in an interior hallway outside the rear of the test cell for protection from physical hazards, electrical hazards, and combustion products.

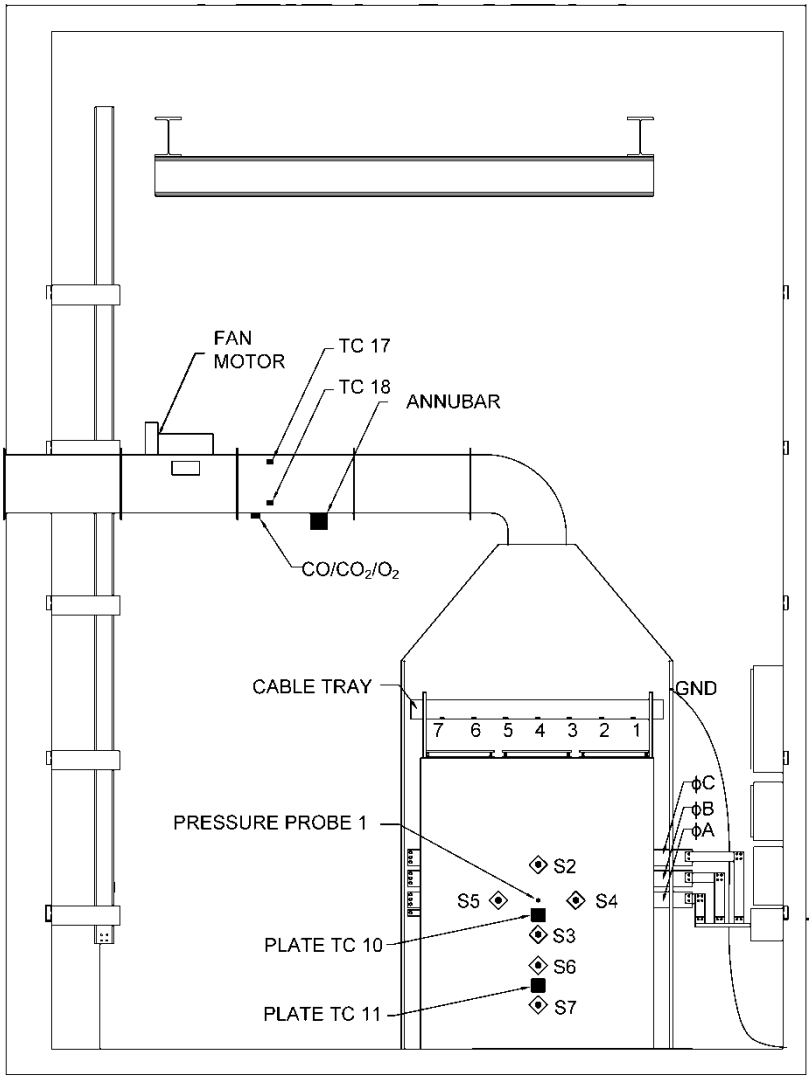

Figure 1 Elevation view of calorimetry hood, enclosure, and instrumentation. Plate thermometers facing downward under cable tray, slug calorimeters denoted by diamond symbols, stack thermocouples denoted by "TC", exhaust gas sampling probe location denoted by "$CO/CO_2/O_2$"; earth ground cable attached to hood denoted "GND", bus bars labeled with phases A, B, and C; not to scale

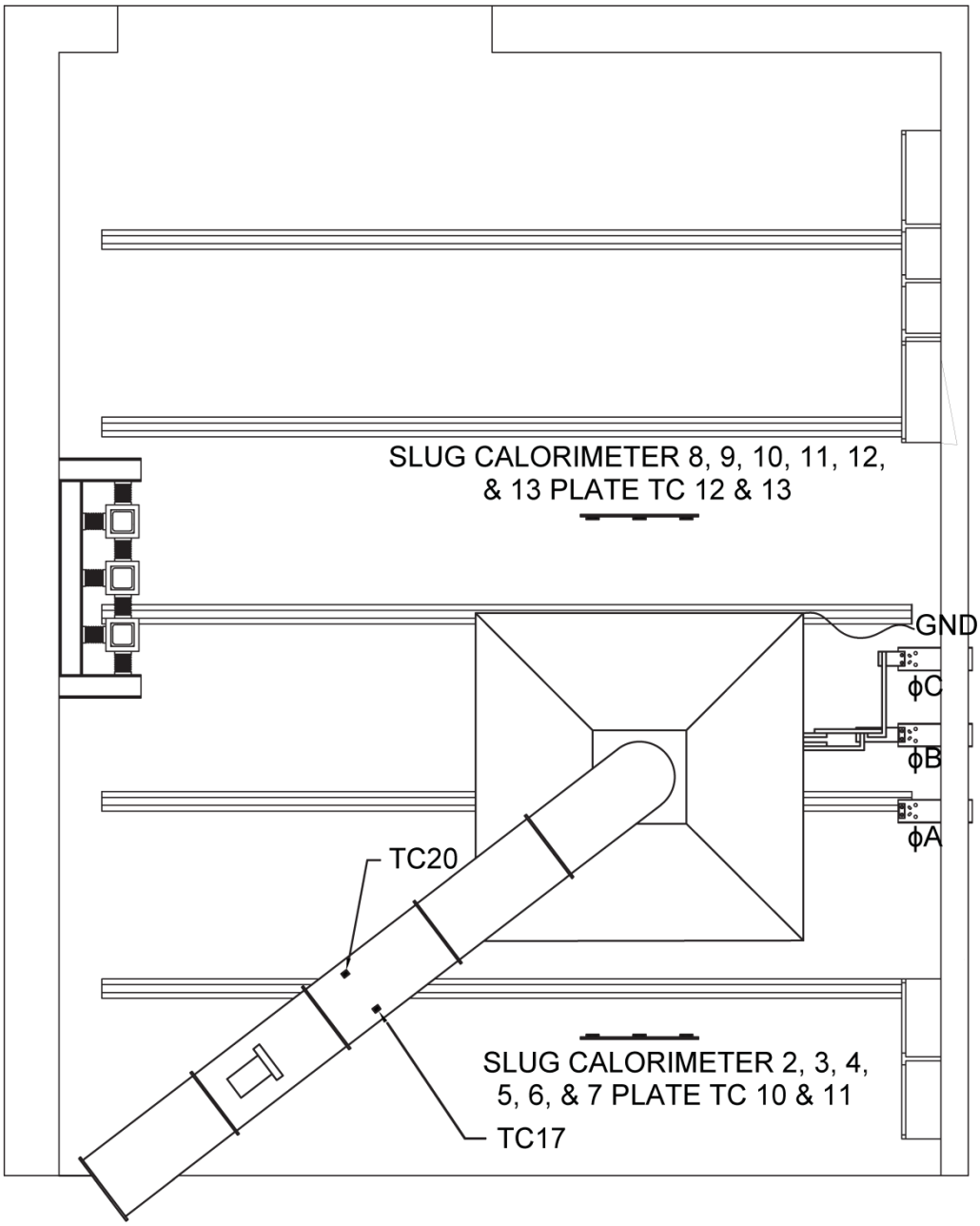

Figure 2 Plan view of calorimetry hood, cabinet, and instrumentation; not to scale

The heat release rates of the ensuing fire, $\dot{Q}(t)$ (kW), was measured by oxygen consumption calorimetry, taking into account the measured concentrations of oxygen, carbon dioxide, and carbon monoxide in the exhaust gas [5], [6].

$$\dot{Q}(t) = \left[E_{O_2}\emptyset - \left(E_{CO} - E_{O_2}\right)\frac{1-\emptyset}{2}\left(\frac{X_{CO}}{X_{O_2}}\right)\right]\frac{\dot{m}_e}{1+\emptyset(\propto -1)}\frac{M_{O_2}}{M_a}\left(1 - X_{H_2O,\infty}\right)X_{O_2,\infty} \quad (1)$$

$$\emptyset = \frac{X_{O_2,\infty}\left(1 - X_{CO_2} - X_{CO}\right) - X_{O_2}\left(1 - X_{CO_2,\infty}\right)}{\left(1 - X_{O_2} - X_{CO_2} - X_{CO}\right)X_{O_2,\infty}} \quad (2)$$

Here $\propto$ is the combustion expansion factor of 1.105, $\emptyset$ is the oxygen depletion factor, E_{O_2} is the net heat released for complete combustion of typical fuels, 13100 kJ/(kg O_2), E_{CO} is the

net heat released for complete combustion of CO, 17600 kJ/(kg O_2), M_a is the molecular weight of incoming air [g/mol], M_{O_2} is the molecular weight of oxygen [g/mol], $\dot{m}_e$ is the exhaust mass flow rate in the duct [kg/s], $X_{O_2,\infty}$ is the initial oxygen volume fraction, X_{O_2} is the measured oxygen volume fraction, $X_{CO_2,\infty}$ is the initial carbon dioxide volume fraction, X_{CO_2} is the measured carbon dioxide volume fraction, X_{CO} is the measured carbon monoxide volume fraction, and $X_{H_2O,\infty}$ is the volume fraction of water vapor.

Due to the large range of possible heat release rates, the apparatus design was biased toward resolution of the relatively small heat release rates expected from the ensuing fires. The heat release rate measurement range for the hood is approximately 10 kW to 3000 kW. The velocity of gases flowing through the hood duct was measured using an Annubar®[1] averaging differential pressure element attached to a differential pressure transducer. The geometry of the duct system differed from that specified by the manufacturer, resulting in less flow straightening and flow development. Due to the difference, calibration fires were used to determine the flow coefficient for the differential pressure element.

Calibration fires were produced by a propane diffusion burner approximately 0.3 m by 0.3 m in size, providing fire heat release rates of approximately 35 kW and 50 kW. The propane burner heat release rates were calculated from the propane heat of combustion and the standard volume of propane provided to the burner as measured by a dry test flow meter corrected for temperature and pressure. For the oxygen consumption calculation of heat release from the propane burner, the value of E_{O_2} for propane is 12.78 MJ/(kg O_2) [7]. The combined standard uncertainty, composed of Type A and Type B uncertainties, in the base heat release measurements was 10 %. The expanded uncertainty in the base heat release measurements was 20 %, with a coverage factor of 2, which corresponds to a confidence interval of 95 % [8], [9].

During the experiments, the effects of wind and smoke escaping the sides of the hood increased the level of measurement uncertainty. The one open side of the test cell allowed prevailing winds to drive combustion products away from the hood. Fire resistant fabric side skirts reduced the loss of smoke, but wind conditions resulted in the loss of significant quantities of smoke in some experiments. For each HEAF fire experiment, additional uncertainty contributions due to wind and losses of combustion products were estimated using observations and video recordings.

Temperature and Heat Flux

One measure of the thermal environment during HEAF events and ensuing fires is the thermal heat flux imposed on materials surrounding the cabinets. There are various techniques available for measuring thermal heat flux, including water cooled transducers, slug calorimeters, directional flame thermometers (DFT), and plate thermometers (PT). The use of these transducers for measuring the heat fluxes in HEAF events was explored in an NRC funded project [10]. For the OECD program HEAF experiments, the choice of transducers was revisited.

The prime considerations for the experiments included a transducer that was sturdy and possessed a relatively short response time. One of the technologies frequently used in fire experiments is the water-cooled heat flux transducer (Schmidt-Boelter and Gardon Gauge types). There are two major drawbacks for their use in HEAF experiments, however. The first drawback is the presence of cooling water in the test cell, which presents logistical complications and safety hazards. The second drawback is related to the dynamic range of the

[1] Certain commercial equipment, instruments, or materials are identified in this paper in order to specify the experimental procedure adequately. Such identification is not intended to imply recommendation or endorsement by the National Institute of Standards and Technology, nor is it intended to imply that the materials or equipment identified are necessarily the best available for the purpose.

sensors. In order to capture the low heat fluxes from small ensuing fires to a reasonable level of uncertainty, a transducer with a measurement range from approximately 10 kW/m^2 to 200 kW/m^2 could be chosen, resulting in an expanded uncertainty of approximately 6 kW/m^2 (coverage factor of 2, 95 % confidence interval). A transducer of this range may be destroyed, however, by the fluxes resulting from impingement of plasma from the arcing portion of the experiment, which may be on the order of 1 MW/m^2. If a transducer with a measurement range high enough to survive the arcing is used, the heat flux measurement uncertainty would be too high for the ensuing fires.

Plate thermometers are robust sensors that can survive in hostile HEAF environments. A plate thermometer similar to that described in the literature [11], [12], and [13] was chosen for heat flux measurements in the OECD experiments due to its rugged construction, low cost, lack of cooling water, and emissivity and convective heat flux coefficients similar to power plant safety-related equipment.

The plate thermometer (PT) from the literature was modified for faster response and simpler manufacture. In order to decrease response time, the specified sheathed thermocouple was replaced by 0.51 mm diameter (24 AWG) Type-K thermocouple wires welded directly to the rear of an Inconel® 600 plate. The thickness of the mineral fiber blanket was increased to approximately 25.4 mm to decrease heat loss. A square plate of Inconel, approximately 100 mm by 100 mm in size, replaces the bent plate to reduce heat losses from the sides and simplify electrical isolation. Machine screws with ceramic washers allow for legs to be attached at the rear of the plate thermometer in order to simplify installation into cable trays and increase locational accuracy. The modified plate thermometer is shown in Figure 3 and Figure 4.

The incident heat flux on a plate thermometer can be calculated from a heat balance using the following relation, a rearrangement of Equation 18 from Ingason and Wickstrom [12]:

$$\dot{q}''_{\text{inc}} = \sigma \cdot T_{\text{PT}}^4 + \frac{(h_{\text{PT}} + K_{\text{cond}})(T_{\text{PT}} - T_\infty)}{\varepsilon_{\text{PT}}} + \frac{\rho_{\text{ST}} \cdot C_{\text{ST}} \cdot \delta \cdot \left(\frac{\Delta T_{\text{PT}}}{\Delta t}\right)}{\varepsilon_{\text{PT}}} \quad (3)$$

Here $\dot{q}''_{\text{inc}}$ is the incident heat flux, σ is the Stefan-Boltzmann Constant, 5.670×10^{-8} W/(m^2·K^4), T_{PT} is the temperature of the plate (K), h_{PT} is the convection heat transfer coefficient, 10 W/(m^2·K), K_{cond} is the conduction correction factor determined from NIST cone calorimeter data, 4 W/(m^2·K), T_∞ is the ambient temperature (K), ε_{PT} is the plate emissivity, 0.85 at 480 °C as rolled and oxidized and specified by the alloy manufacturer, ρ_{PT} is the alloy plate density, 8470 kg/m^3 from the alloy manufacturer, C_{ST} is the alloy plate heat capacity, 502 J/(kg·K) at 300 °C from the alloy manufacturer, δ is the alloy plate thickness, 0.79 mm, and Δt is the data acquisition time step of 0.2 s.

The modified PTs were heated in the cone calorimeter [14] to verify their performance and the fit of the simple thermal model in Equation (3). The plates were tested from 5 kW/m^2 to 75 kW/m^2 by heating from ambient temperature to steady state and then allowing them to cool. At a steady state flux of 75 kW/m^2 the calculated heat flux reached 63 % of the incident heat flux in approximately 0.7 s. The combined standard uncertainty in steady state heat flux measured by the plate thermometers, composed of Type A and Type B uncertainties, is 2.5 % at 75 kW/m^2. The expanded uncertainty in the steady state heat flux measurement is 5 % at 75 kW/m^2, with a coverage factor of 2 which corresponds to a confidence interval of 95 % [8].

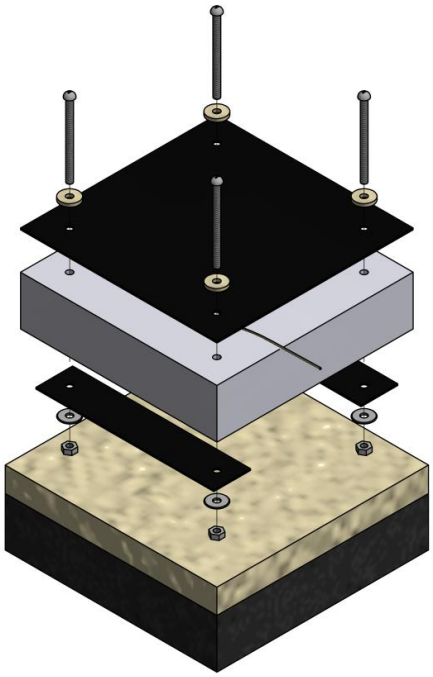

Figure 3 Exploded view of modified plate thermometer with cone calorimeter sample holder

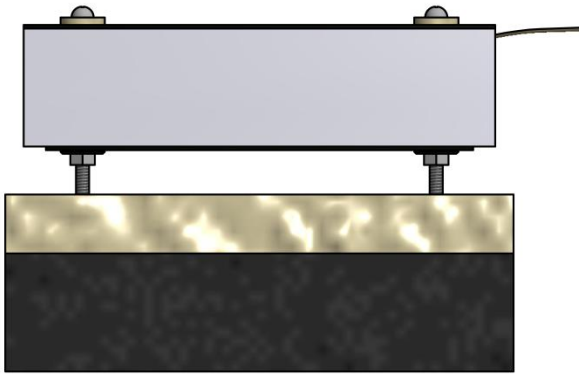

Figure 4 Elevation view of modified plate thermometer on cone calorimeter sample holder

The heating of plate TCs in the cone calorimeter was modeled in one dimension with the Fire Dynamics Simulator (FDS) [15] to verify the assumptions and property data. Agreement to within 1 % was found between the temperatures measured during exposure in the cone calorimeter and the FDS predicted temperatures. Data from heating the plate thermometer at 75 kW/m^2 in the cone calorimeter is included in the FDS validation library.

Sensor Wiring and Data Acquisition

Due to the voltages, currents, and electrical arcing that are present in and around the electrical equipment used in the HEAF experiments, electromagnetic interference (EMI) was present in the test facility. The electric and magnetic fields are capable of inducing voltages and currents in the sensor and data acquisition wiring. In order to reduce the effects of EMI, several strategies were employed in concert: shielding, isolation, signal conditioning, grounding, and electrical power conditioning. This multi-faceted approach greatly reduced or eliminated the effects of EMI on the measurement results.

A conceptual drawing of the sensors, instrumentation, and data acquisition is shown in Figure 5 and Figure 6. Figure 5 shows the wiring concept for a typical sensor, which includes plate thermometers and thermocouples. Figure 6 shows the wiring concept for the gas analyzers and differential pressure transducer for measuring hood flow rates.

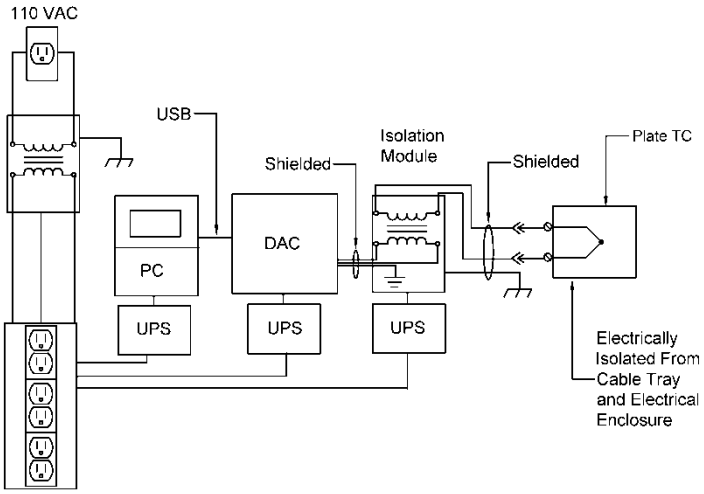

Figure 5 EMI resistant wiring concept for plate thermometer measurements

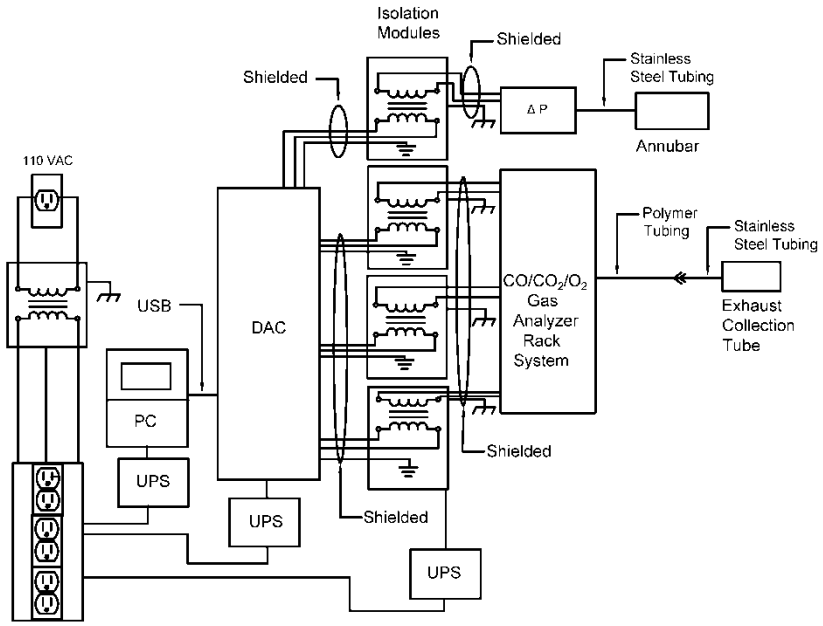

Figure 6 EMI resistant wiring concept for gas analysis and hood flow measurements

The sensor extension wiring is shielded, with the shield grounded near the sensor to earth ground. The sensor extension traveled through the test cell, via a route as far away from the current supply bus bars as practicable, through the back wall of the test cell, and to a signal conditioner and isolation transformer (isolation module). Each sensor channel had a dedicated isolation module. For thermocouple channels, the isolation modules also converted the low level mV signal produced by the thermocouple to a high level signal (0 VDC to + 5 VDC) linearized for a temperature range of – 100 °C to 1350 °C using a simulated ice junction.

Non-thermocouple sensors were served by isolation modules that converted the input signals to ± 1 VDC or ± 5 VDC output signals.

The output of each isolation module was connected to one of two data acquisition modules, housed in a separate enclosure, via a shielded cable that was grounded to earth ground. The high level signals from the isolation modules were sampled by the data acquisition system (DAC), with the results communicated to a laptop computer (PC) via a USB cable. Data were recorded by the data acquisition system at a rate of 5 Hz.

The main 115 VAC building power for the PC, data acquisition system, isolation modules, gas analyzers, and pressure transducer was supplied through signal conditioners, uninterruptible power supplies, and isolation transformers. The equipment chassis were grounded to earth. The heat release rate hood and duct support scaffolding were also grounded to earth. Grounding all of the equipment and cable shielding to the same earth ground prevented ground loops. The cable trays above the electrical enclosures were electrically isolated from the enclosure and hood and ungrounded. The enclosures were supplied with 3 phase power in a delta configuration, with the enclosure ungrounded.

RESULTS

Heat Release Rate

During the arcing phase of the HEAF experiments it was common for large quantities of rapidly generated combustion products to escape the measurement hood to the atmosphere and therefore avoid measurement. In order to measure heat release rate during the arcing phase, a larger hood would be needed to capture the combustion products, the size of which is impractical for a portable system. To measure larger fires, the exhaust mass flow rate would need to be increased, which would decrease the ability to resolve small fires, and increase measurement uncertainty. The purpose of the portable apparatus is to measure the HRR of the secondary phase of the HEAF event, i.e., the ensuing fire.

Oxygen consumption calorimetry for ordinary combustible materials such as flammable gases, flammable and combustible liquids, wood, and polymers utilizes a heat content of approximately 13.1 MJ/kg of oxygen consumed [5]. During the HEAF portion of the experiments, a significant quantity of copper and aluminum were oxidized. The heat release rate calculations do not take into account the difference in E_{O2} between oxidation of metals and the combustion of ordinary combustibles. During the HEAF portion of the experiments, the average heat release rate [MW] was estimated from the arc energy [MJ] divided by the arc duration (s) instead of oxygen consumption calorimetry.

The HEAF and ensuing fire from an experiment in a medium voltage cabinet are shown in Figure 7 and Figure 8. The nominal cabinet operating conditions were 7200 VAC and 24 kA with an arc of approximately 2554 ms in duration. The initial heat release from the cabinet due to the arc was not fully captured, but may be estimated as an average of approximately 28 MW from the arc energy expended during the arc. The heat release rate of the ensuing fire that occurred in the electrical enclosure following the HEAF event was recorded, with the primary fuel load consisting of the breaker housing. The maximum heat release rate of the ensuing fire was 165 kW. The expanded uncertainty in the heat release measurement is 25 %, with a coverage factor of 2, which corresponds to a confidence interval of 95 %.

Figure 7 Medium voltage HEAF

Figure 8 Ensuing fire

Temperature and Heat Flux

A low voltage HEAF in an enclosure with nominal operating conditions of 480 VAC and 50 kA with an arc of approximately 2115 ms in duration is shown in Figure 9 and Figure 10. The locations of the plate thermometers installed in the experiment are shown in Figure 1 and Figure 2. The temperatures reported by the thermocouples attached to the back of the nickel alloy plates of the modified plate thermometers are shown in Figure 11 and Figure 12.

Figure 9 Low voltage HEAF; front of cabinet

Figure 10 Low voltage HEAF; top of cabinet; cable tray visible in upper right of photo

During some of the experiments, plate thermometers were directly impacted by plasma ejected from the cabinet. This contact resulted in abnormal thermocouple voltages and therefore to abnormal temperature change readings from the thermocouples. The resulting abnormal voltages, temperatures, and heat fluxes could be positive or negative. The data from plate TCs directly impacted by plasma could be used outside of the time where the arc was present by using the plate TC equations. An average heat flux during the arc can be calculated by treating the plate as a well-insulated, thermally-thin solid.

The heat flux histories of the plate thermometers in the low voltage experiment were calculated from the temperature data and are shown in Figure 13 and Figure 14. In this particular case, the plasma generated by the arc event did not cause significant abnormal voltages. The peak incident heat flux measured approximately 0.9 m (3 ft) from the cabinet at PT location 10 was 17 kW/m^2 during this experiment. The peak incident heat flux measured in the cable tray located approximately 0.3 m (1 ft) above the cabinet at PT location 5 was 72 kW/m^2 during this experiment.

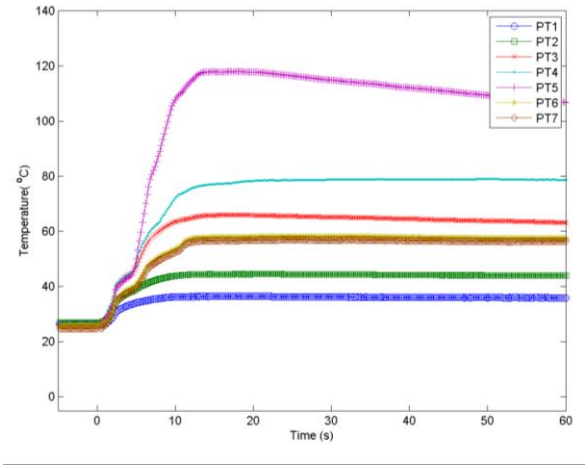

Figure 11 Cable tray plate thermometer temperatures, low voltage test. Temperature expanded uncertainty of ±3°C with coverage factor of 2

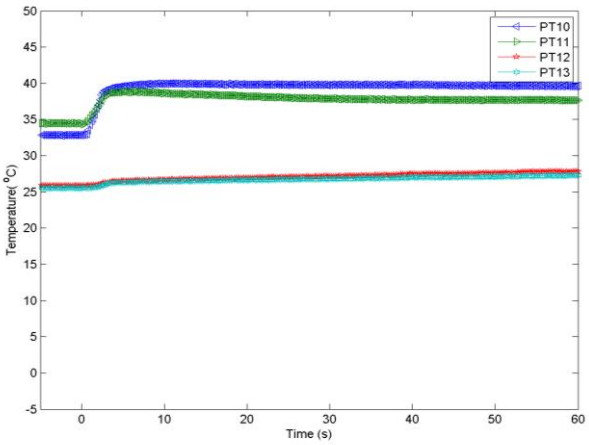

Figure 12 Vertical plate thermometer temperatures, low voltage test. Temperature expanded uncertainty of ±3°C with coverage factor of 2

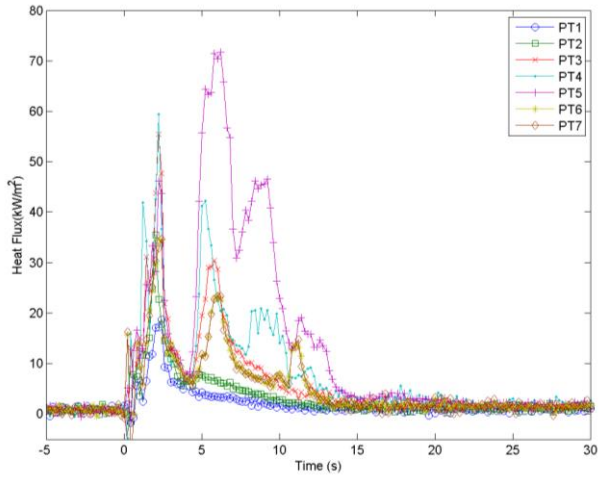

Figure 13 Cable tray PT heat flux, low voltage test; heat flux expanded uncertainty of ±4 kW/m^2 at 75 kW/m^2 with coverage factor of 2

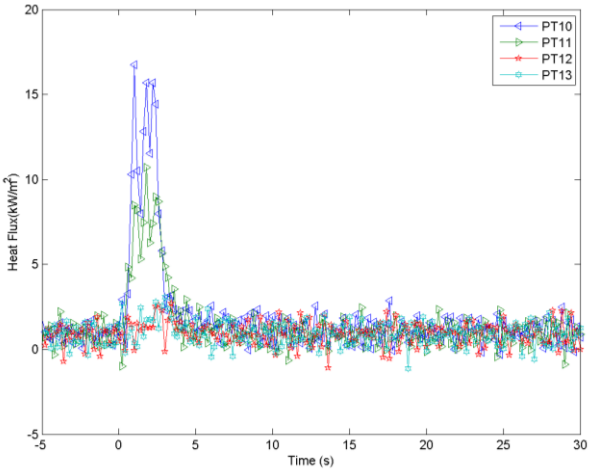

Figure 14 Vertical PT heat flux, low voltage test; heat flux expanded uncertainty of ±4 kW/m^2 at 75 kW/m^2 with coverage factor of 2

The Fire Dynamics Simulator [15] was used to simulate the one dimensional heating of a plate thermometer (PT5 above) exposed to the heat flux history calculated from the plate thermometer measurement, Equation 3. The experimentally measured plate temperature and the corresponding FDS prediction agreed to within 2 %, which serves as verification of the method to calculate the heat flux from the measured plate temperature.

The test facility provided slug calorimeters for the measurement of the incident energy; that is, the total energy absorbed by thermally-thin targets at various locations around the enclosure. The incident energy was calculated from the temperature history according to standard methods [16]. The measurements from the slugs were also found to be adversely affected by direct impingement of plasma exiting the cabinets. The incident energy during the arc

phase of the 480 V experiment was approximately 31 kJ/m^2 (0.75 cal/cm^2), measured at Slug 2.

CONCLUSIONS

The portable oxygen consumption calorimetry hood is effective for measuring the heat release rate of HEAF ensuing fires. As expected, HEAF arcing events produce too much effluent to be captured by the hood as designed. The average energy release rate during the arcing period, however, can be estimated from the electrically measured arc energy and arc time.

Plate TCs are an effective method for characterizing the thermal assault on NPP cable trays and equipment, and can serve as input boundary conditions for FDS modeling of target objects. Data during the arc event may need to be averaged over the time of the arc if plasma impingement on the plate TC causes abnormal signals.

ACKNOWLEDGEMENTS

The authors are grateful for the support of the participating OECD/NEA member countries, the OECD HEAF Project members, and the OECD/NEA. The authors also acknowledge the contributions of the other members of the NIST experimental team: Mr. Michael Selepak and Mr. John “Randy” Shields. Mr. Edward Hnetkovsky is acknowledged for fabrication of equipment and sensors. The authors are grateful to Dr. Kevin McGrattan of NIST for providing simulations of the plate TCs heated in the cone calorimeter and the HEAF experiment. Mr. Benjamin Lee of BSI is acknowledged for the calorimetry hood drawings included in this paper. Mr. David Stroup of NRC is gratefully acknowledged for serving as the NRC Project Manager for the NIST research effort. The authors are grateful to Mr. Mark Henry Salley of NRC for envisioning the cooperative relationship between NRC, OECD/NEA, and NIST for studying HEAF phenomena.

REFERENCES

[1] Organisation for Economic Co-operation and Development (OECD) Nuclear Energy Agency (NEA), Committee on the Safety of Nuclear Installations (CSNI), *OECD FIRE Project - Topical Report No. 1, Analysis of High Energy Arcing Fault (HEAF) Fire Events*, NEA/CSNI/R(2013)6, Paris, France, June 2013, http://www.oecd-nea.org/nsd/docs/2013/csni-r2013-6.pdf.

[2] Electric Power Research Institute (EPRI) and United States Nuclear Regulatory Commission Office of Nuclear Research (NRC-RES), *Fire PRA Methodology for Nuclear Power Facilities,* EPRI/NRC-RES, Final Report, Volume 2: Detailed Methodology, EPRI 1011989, NUREG/CR-6850, Palo Alto, CA, and Rockville, MD, USA, September 2005, http://www.nrc.gov/reading-rm/doc-collections/nuregs/contract/cr6850/.

[3] Organisation for Economic Co-operation and Development (OECD) Nuclear Energy Agency (NEA), Committee on the Safety of Nuclear Installations (CSNI), Working Group IAGE (WGIAGE), *OECD NEA CSNI WGIAGE Task on High Energy Arcing Fault Events (HEAF)*, Task Report, NEA/CSNI/R(2015)10, Paris, France, 2015, https://www.oecd-nea.org/nsd/docs/2015/csni-r2015-10.pdf.

[4] McGrattan, K., S. Bareham, *Heat Release Rates of Electrical Enclosure Fires (HELEN-FIRE) - Draft Report for Comment,* NUREG/CR-7197*,* Nuclear Regulatory Commission (NRC), Office of Nuclear Regulatory Research, Division of Risk Analysis, Washington, DC, USA, 2015, http://www.nrc.gov/reading-rm/doc-collections/nuregs/contract/cr7197/.

[5] ASTM International, *Standard Practice for Full-Scale Oxygen Consumption Calorimetry Fire Tests*, ASTM Standard E2067-12, West Conshohocken, PA, USA, 2012, http://www.astm.org/Standards/E2067.htm.

[6] International Organization for Standardization, *BS ISO 5660-1:2015, Reaction to fire tests - Heat release, smoke production and mass loss rate - Part 1: Heat release rate (cone calorimeter method) and smoke production rate (dynamic measurement*), Geneva, Switzerland, March 2015, http://www.iso.org/iso/home/store/catalogue_tc/catalogue_detail.htm?csnumber=57957.

[7] DiNenno, P. J., Ed., *SFPE Handbook of Fire Protection Engineering*, 4th ed., Society of Fire Protection Engineers (SFPE), Bethesda, MD, USA, National Fire Protection Association (NFPA), Quincy, MA, USA, 2008, http://catalog.nfpa.org/SFPE-Handbook-of-Fire-Protection-Engineering-P13936.aspx?icid=D482.

[8] Taylor, B.N. and C. E. Kuyatt, *Guidelines for Evaluating and Expressing the Uncertainty of NIST Measurement Results*, NIST Technical Note 1297, National Institute of Standards and Technology (NIST), Gaithersburg, MD, USA, 1994, http://www.nist.gov/pml/pubs/tn1297/.

[9] Lafarge, T. and A. Possolo, "The NIST Uncertainty Machine", in: *NCLSI Measure J. Meas. Sci.*, to be published September 2015.

[10] Lopez, C., W. B. Wente, and V. G. Figueroa, *Evaluation of Select Heat and Pressure Measurement Gauges for Potential Use in the NRC/OECD High Energy Arc Fault (HEAF) Test Program*, Sandia National Laboratories (SNL), Albuquerque, NM, USA, 2014.

[11] Haggkvist, A., J. Sjostrom, and U. Wickstrom, "Using plate thermometer measurements to calculate incident heat radiation", *Journal of Fire Sciences*, Vol. 31, No. 2, 2013, pp. 166-177.

[12] Ingason, H. and Wickstrom, U., "Measuring incident radiant heat flux using the plate thermometer," *Fire Safety Journal*, Vol. 42, No. 2, 2007, pp. 161-166.

[13] Wickstrom, U., "The Plate Thermometer - A simple instrument for reaching harmonized resistance tests," *Fire Technology*, Vol. 30, No. 2, 1994, pp. 209-231.

[14] ASTM International, *Standard Test Method for Heat and Visible Smoke Release Rates for Materials and Products Using an Oxygen Consumption Calorimeter*, ASTM Standard E1354-15, West Conshohocken, PA, USA, 2015, http://www.astm.org/Standards/E1354.htm.

[15] McGrattan, K., et al., *Fire Dynamics Simulator, Technical Reference Guide*, Sixth Edition, NIST Special Publication 1018, Vol. 1: Mathematical Model; Vol. 2: Verification Guide; Vol. 3: Validation Guide; Vol. 4: Configuration Management Plan, National Institute of Standards and Technology (NIST), Gaithersburg, MD, USA, and VTT Technical Research Centre of Finland, Espoo, Finland, November 2013, http://firemodels.github.io/fds-smv/.

[16] ASTM International, *Standard Test Method for Determining the Arc Rating of Materials for Clothing*, ASTM Standard F1959 / F1959M-14, West Conshohocken, PA, USA, 2014, . http://www.astm.org/Standards/F1959.htm.